Effect of Mechanical Stretching on DNA Conductance

Christopher Bruot, Limin Xiang, Julio L. Palma, and Nongjian Tao*

Center for Bioelectronics and Biosensors, Biodesign Institute, School of Electrical, Energy and Computer Engineering, Arizona State University, Tempe, Arizona 85287-5801, United States

ABSTRACT Studying the structural and charge transport properties in DNA is important for unraveling molecular scale processes and developing device applications of DNA molecules. Here we study the effect of mechanical stretching-induced structural changes on charge transport in single DNA molecules. The charge transport follows the hopping mechanism for DNA molecules with lengths varying from 6 to 26 base pairs, but the conductance is highly sensitive to mechanical stretching, showing an abrupt decrease at surprisingly short stretching distances and weak dependence on DNA length. We attribute this force-induced conductance decrease to the breaking of hydrogen bonds in the base pairs at the end of the sequence and describe the data with a mechanical model.

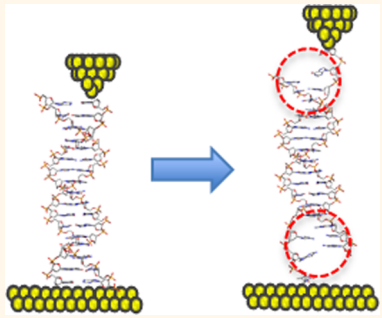

KEYWORDS: molecular electronics · single molecule · DNA conductance · mechanical properties · STM · break junction

Studying charge transport in DNA (dsDNA) is fundamental to understanding relevant biological processes and developing electronic devices with DNA molecules.[1−3] Evidence has shown that charge transport in dsDNA molecules is mediated by the $\pi-\pi$ stacking interactions between neighboring base pairs.[4−9] These $\pi-\pi$ stacking interactions are sensitive to structural changes in dsDNA molecules, which can be induced by stretching the molecules mechanically.[10−12] Indeed, it has been shown that DNA undergoes a structural transition when mechanically stretched,[13−17] which has been attributed to either a reversible configuration change from native form (B-DNA) to stretched form (S-DNA) or irreversible force-induced melting.[18−24] During both processes, the $\pi-\pi$ stacking interactions are expected to be seriously disrupted, leading to a large change in the charge transport of DNA. Despite the intensive study of mechanical properties of DNA, the effect of mechanical stretching on charge transport in dsDNA molecules has not been investigated.

Here we describe a study of mechanical stretching effect on charge transport in dsDNA molecules using a scanning tunneling microscope (STM) break junction technique[25] in the native aqueous environment of DNA. The dsDNA molecules are terminated with linkers such that they can bridge between the STM tip (gold) and substrate (gold) electrodes. Separating the tip and substrate electrodes, the dsDNA molecule is stretched while the conductance is continuously measured. By analyzing the evolution of single-molecule conductance during electrode separation, the effect of the stretching transition on dsDNA conductance is studied for dsDNA molecules with lengths varying from 6 base pairs (~2 nm) to 26 base pairs (~9 nm). The dsDNA resistance is found to increase linearly with the length, consistent with thermally activated hopping transport,[26] in which holes hop sequentially along the molecule *via* the stacked base pairs. However, the charge transport in DNA is highly sensitive to mechanical stretching, showing an abrupt decrease in conductance at surprisingly short stretching distances, which is weakly dependent on the molecular length. These unexpected observations are attributed to a force-induced melting mechanism[27] and are consistent with simulations[24] and de Gennes' DNA ladder model[23] for dsDNA mechanics.

RESULTS AND DISCUSSION

The dsDNA molecules studied here are all self-complementary strands denoted as 5′-A$(CG)_N$T-3′ (N = 2−12). The thymine and adenine bases at the 3′ and 5′ ends (respectively) are used to prevent mismatch.

* Address correspondence to nongjian.tao@asu.edu.

Received for review November 3, 2014 and accepted December 21, 2014.

Published online December 21, 2014
10.1021/nn506280t

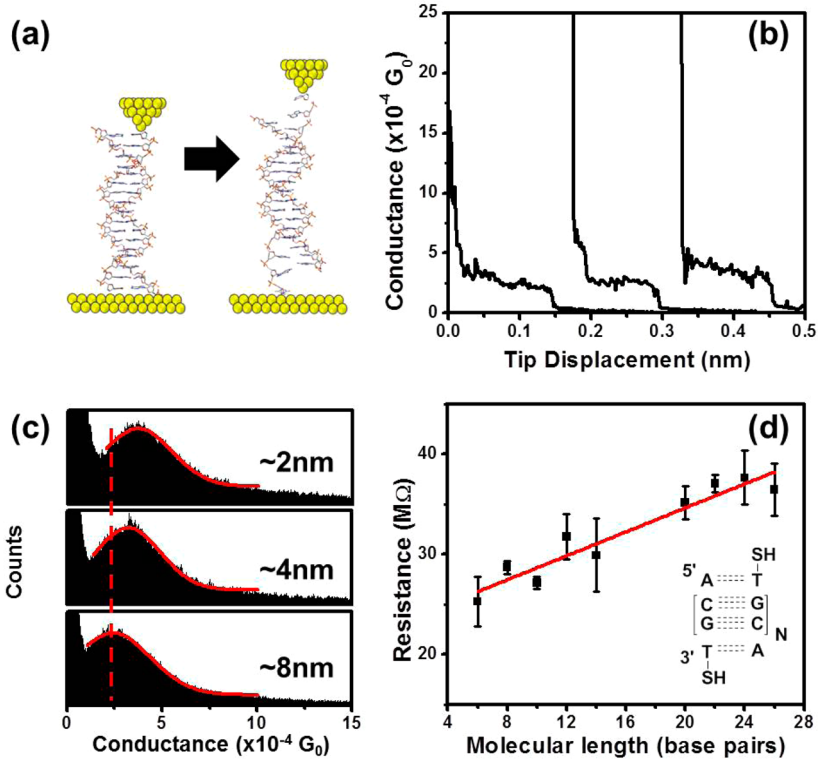

Figure 1. dsDNA molecular conductance. (a) Cartoon illustrating the STM break junction experimental technique. The top electrode is an STM tip, and the bottom electrode is an STM substrate. The tip contacts molecules bound to the substrate. The current is measured while the tip is retracted. (b) Examples of conductance *vs* tip displacement curves for the 14 base pair dsDNA molecule. Curves are offset on the *x*-axis for clarity. (c) Conductance histograms with Gaussian fittings for 5′-A(CG)$_2$T-3′, 5′-A(CG)$_5$T-3′, and 5′-A(CG)$_{12}$T-3′ base pair (bottom to top, respectively). Red dotted line intended to guide the eye. (d) Average resistance *vs* molecular length for all molecules studied. Red line is linear fitting intended to guide the eye. Inset shows structure of molecules.

The dsDNA molecules are linked to the gold electrodes (STM tip and substrate) through an alkanethiol linker, which attaches to the deoxyribose ring at the 3′ end (see Supporting Information). As a control experiment, an amine linker is also studied (see Supporting Information). Details of molecular preparation and annealing are presented in the Methods section.

The experimental setup is illustrated in Figure 1a. Briefly, a gold STM tip, coated with an insulation layer, is brought into contact with a gold substrate in the presence of the dsDNA molecule. A small bias voltage applied between the tip and substrate causes a current between the two electrodes when the separation between them is small. The tip is then retracted while the current is monitored. In the absence of a molecule bridging the tip and substrate, the current decays exponentially with tip retraction, as expected for a tunnel junction. However, when a molecule bridges the tip−substrate gap, a plateau is seen in the current *versus* tip displacement, as shown in Figure 1b, which represents a single-molecule bridging the tip−substrate gap. Measuring the dependence of the plateau current on stretching allows us to study the effect of mechanical stretching on charge transport in dsDNA. This process can be repeated thousands of times, and statistical analysis of these current *versus* displacement curves results in a conductance histogram, from which the most probable conductance for a single molecule is determined (Figure 1c).

Figure 1d shows the dependence of the measured dsDNA resistance (inverse of conductance) on molecular length ranging from 6 to 26 base pairs. Over this wide range of molecular length, the resistance is linearly proportional to molecular length, indicating a thermally activated hopping process.[28] As opposed to transport through the tunneling mechanism, which has an exponential dependence on molecular length, this hopping process is characterized by weak length dependence, given by[29]

$$R \propto \frac{1}{k_L} + \frac{1}{k_R} + \frac{N-1}{k} \qquad (1)$$

where $k_{L(R)}$ is the charge transfer rate between the left (right) electrode and the nearest molecular hopping site and k is the charge transfer rate between hopping sites on the molecular bridge. The ratio between the intercept and slope in eq 1, $(k_L^{-1} + k_R^{-1})/k^{-1}$, measures the relative importance of the contact, that is, hopping between the electrodes and the nearest molecular hopping sites. Equation 1 fits the experimental data well, and the ratio between the intercept and slope is ∼40. This large value suggests that the resistance of

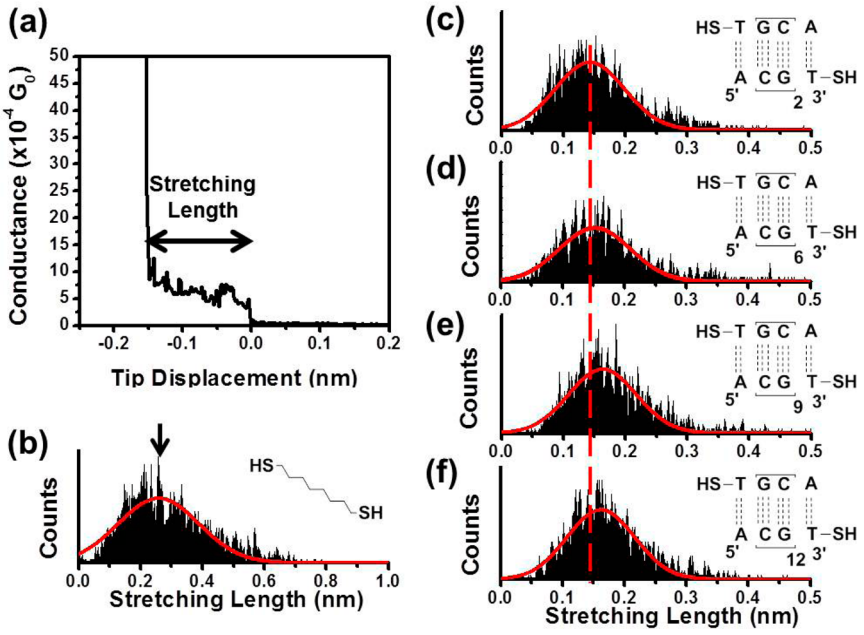

Figure 2. Molecular junction stretching length. (a) Example conductance *vs* tip displacement curve for the dsDNA sequence 5′-S(CG)$_2$T-3′, illustrating the stretching length measurement technique. (b) Stretching length histogram with Gaussian fit for octanedithiol. Arrow indicates peak position. (c–f) Stretching length histograms with Gaussian fit for 5′-A(CG)$_2$T-3′, 5′-A(CG)$_6$T-3′, 5′-A(CG)$_9$T-3′, and 5′-A(CG)$_{12}$T-3′ molecules, respectively (dsDNA molecules have 6, 14, 20, and 26 base pairs, respectively). Drawings of the respective molecular structures are inset to the histograms. Red dotted lines are intended to guide the eye.

dsDNA, or the rate-limiting step, is determined by the contact transfer rates, $k_{L(R)}$, and the base to base transfer rate, k, is roughly 40 times more efficient. This observation supports long-range charge transport in DNA.[30,31]

The spring constants of dsDNA molecules studied here range from ∼0.5 to 0.1 N/m (for 6 base pairs to 26 base pairs, respectively),[32] soft when compared to the Au–Au bond (∼8 N/m), which is known to be the softest part of the thiol–gold linker.[33] Thus, we expect the dsDNA molecules, rather than the contacts, to be substantially stretched when separating the two electrodes apart. Considering the transport model above, one would expect the conductance to decrease as the dsDNA molecule is stretched because of the increase in the distance between neighboring bases, which will be accompanied by a decrease in electronic coupling. Indeed, as can be seen in Figure 1b, a decrease in conductance with tip displacement is observed upon initial stretching in many dsDNA molecular junctions, suggesting that initially the conductance change with stretching is caused by the decrease in coupling between neighboring bases. However, following the initial slow conductance decrease, there is an abrupt decrease in conductance, indicating a structural transition in the electrode–dsDNA–electrode junction.

An important parameter that characterizes the structural transition is the distance over which the junction can be stretched before the abrupt decrease in conductance or simply stretching length, as illustrated in Figure 2a. As a control experiment, we first examine the stretching length for octanedithiol molecules, consisting of a saturated carbon chain terminated with two thiol linkers that bind to the tip and substrate electrodes. Figure 2b shows that the stretching length for octanedithiol follows a Gaussian distribution with an average value of ∼0.23 nm, close to the distance required to break a gold atomic contact.[33] Previous studies have indeed shown that the Au–Au bond at the contacts breaks first when stretching an octanedithiol junction.[34] This is because the Au–Au bond is the softest and weakest link in the octanedithiol molecular junction. However, analysis of the stretching length for dsDNA molecules yields several surprising observations. First, as shown in Figure 2c, the average stretching length is about 0.14 nm for a 6 base pair dsDNA, much smaller than the length required for breaking the Au–Au bond. This short stretching length shows that, in the case of dsDNA, the thiol–gold linker is not responsible for the abrupt decrease in conductance. Instead, the unique mechanical properties of dsDNA must be responsible for the remarkable short stretching length. To confirm this, we perform a second control experiment by measuring the stretching length of amine-terminated dsDNA molecules. The amine–gold bond is much weaker than the thiol–gold bond and for alkanedithiol molecules has been shown to have much smaller step lengths.[35] However, the measured stretching length of amine-terminated dsDNA is similar to that of thiol-terminated dsDNA (see Supporting Information), confirming that the unanticipated short step length is due to stretching the dsDNA

molecule. The second surprising observation is that the stretching length of dsDNA depends on molecular length weakly (see Figure 2c–f). While dependence on the molecular length is consistent with mechanical stretching of the dsDNA, rather than the contacts, the stretching length increases by only ~0.03 nm from 6 to 26 base pairs, which is counterintuitive based on the following consideration. According to eq 1, the mechanical stretching-induced resistance change is proportional to molecular length (N) given by

$$\Delta R \propto (N-1)\Delta\frac{1}{k} \tag{2}$$

indicating that the stretching length scales with molecular length. This is in contradiction with the experimental data, which reveal very little dependence of the stretching length on molecular length.

The above model assumes that the mechanical stretching is evenly distributed along the dsDNA chain, which we believe is the reason for its discrepancy with the experimental observations. Alternatively, de Gennes[23] developed a DNA ladder model to show that the shear force in dsDNA molecules is distributed over only a few base pairs at the end of the sequence (Figure 3a). This way, if we assume that most of the stretching takes place at the base pairs near the two ends of the dsDNA molecule, the change in resistance depends on both the base–base transfer rate (k) and the electrode–base transfer rate ($k_L = k_R = k_{end}$) so that eq 2 can be rewritten as

$$\Delta R \propto 2\Delta'\frac{1}{k_{end}} + (N-3)\Delta\frac{1}{k} \tag{3}$$

where the first term represents change in the resistance due to the stretching of the end base pairs and the second term is the change in the middle section of the dsDNA. When the stretching is large enough, one of the end base pairs ruptures first (the first term of eq 3), causing the abrupt conductance decease observed here. This model explains naturally the experimental observations, as the stretching length is a measure of the displacement needed to reach the threshold base pair rupture force and is also supported by experiments, simulations, and theories of mechanical properties of dsDNA. For example, Hatch *et al.*[20] used force spectroscopy to show that the shear force is distributed mostly at the end of dsDNA sequences. In addition, simulations by Nath *et al.*[24] recently showed that ~50% of the stretching was localized at the last base pairs at the ends.

On the basis of the above analysis, we use a spring-in-series model, in which the end springs, representing the end base pairs, have a smaller spring constant than the middle. From this model, the stretching length can be expressed as

$$\Delta z = \left[\frac{2}{\alpha_{end}} + \frac{N-3}{\alpha}\right]F \tag{4}$$

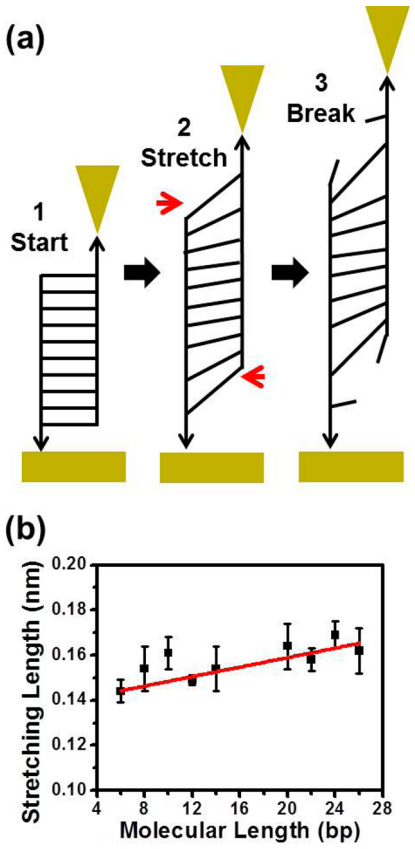

Figure 3. Molecular length effect. (a) Illustration of the evolution of dsDNA molecules during stretching using the de Gennes model. From left to right, the molecular junction is created (1), then stretching initially distorts the base pairs in a non-uniform way (2) until the base pairs at the end break, decreasing the conductance (3). (b) Average stretching length *vs* molecular length for dsDNA molecules studied showing small increase with distance. Red line is fitting of data to a spring-in-series model.

where α_{end} is the end base pair spring constant, α is the spring constant associated with the middle base pairs, and F is the force applied to the molecule. In this model, the measured stretching length is equal to Δz when the force reaches the threshold for breaking the end base pairs, causing the abrupt decrease in conductance. Figure 3b shows the measured stretching length of dsDNA *versus* molecular length and fitting of the experimental data to eq 4. The fitted ratio of the spring constants between the different sections, α/α_{end}, is found to be 70, agreeing with the assumption that the end base pairs are much softer. Assuming the spring constant for middle base pairs measured by Noy *et al.*[32] (~2.8 N/m per base pair), we find that the force applied to the molecule when the conductance decreases is ~3 pN. The threshold force estimated in this way is in good agreement with the force required to break the hydrogen bonds between base pairs, as has been measured with force spectroscopy methods by Hatch *et al.*[20]

Based on the above model, the breaking of the hydrogen bonds of the base pairs near the ends by

the external shear force will abruptly decrease the coupling between the dsDNA hopping sites and the electrodes, resulting in a decrease in the electrode−molecule transfer rate ($k_{L(R)}$ in eq 1) and a sudden decrease in conductance. Thus, the stretching length is a measure of the distance required to break the end base pairs of the dsDNA molecule. The small tip displacement required to achieve the abrupt decrease in conductance and the weak dependence of stretching length on molecular length are a result of the uneven distribution of the displacement across the dsDNA molecule and the relatively weak hydrogen bonds in the end base pairs.

To further ensure that the abrupt decrease in conductance of dsDNA is caused by the rupture of the end hydrogen bonds and not a structural transition in the dsDNA molecule like the B−S transition, we developed a method to stretch and compress single dsDNA molecules repeatedly while monitoring conductance (Figure 4). First the STM break junction method is used to create a molecular junction and then stretch the DNA molecule over a relative short distance, stopping at a position marked by red circle in Figure 4a.[36] After the tip is pushed back toward the substrate (gray line) to compress the molecule, it retracts again to stretch the molecule (black line), by a distance greater than 0.15 nm, until it breaks down, as marked by a red arrow. The tip is then pushed (gray line, Figure 4b) and retracted (black line, Figure 4b) again. The experiment shows that the conductance is reversible if stretching the dsDNA over a short distance. However, the process is irreversible if the molecule is stretched over a large distance such that the abrupt conductance decrease takes place.

The observation above is supported by statistical analysis of ~50 measurements, plotted as a two-dimensional histogram in Figure 4c, showing three distinct sections. In the first section ("I"), the conductance changes exponentially with the tip−substrate separation, signaling that the transport is dominated by tunneling through the solvent when the tip is extremely close to the substrate. Similar characteristics for region I are found for other dsDNA molecules and octanedithiol (see Supporting Information). The second section ("II") is the plateau region, corresponding to the formation and stretching of the molecular junction. This plateau behavior is consistent with the slowly decreasing conductance associated with the initial elongation of the dsDNA molecules discussed above, before the abrupt decrease in conductance. Upon sufficient stretching, however, it enters the third region ("III"), in which the conductance decreases abruptly and irreversibly. For a conformational B−S transition, we would expect the conductance changes to be reversible during the second compression/stretching cycle.[18,19,37,38] The lack of reversibility further indicates that the process responsible for the abrupt decrease in conductance is force-induced melting of the hydrogen bonds in the end base pairs.

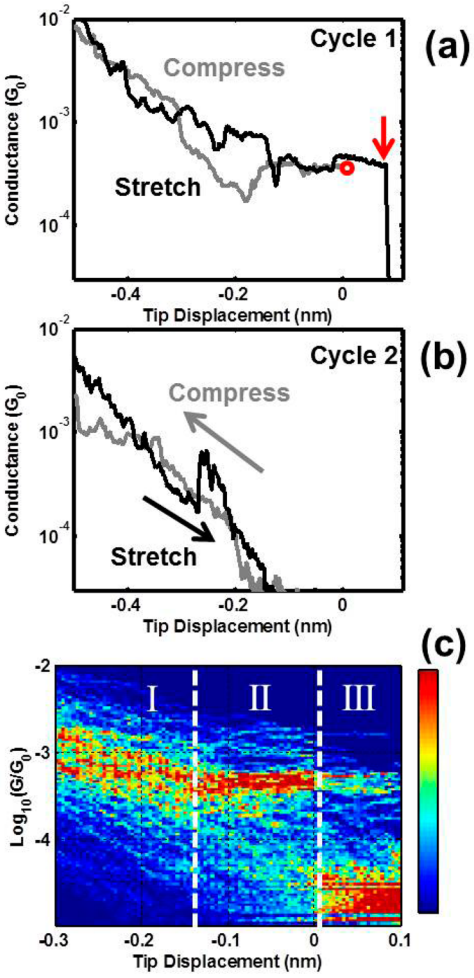

Figure 4. Reversible stretching and compressing for 5′-A(CG)$_6$T-3′. (a) Example conductance *vs* tip displacement curve during the first compressing/stretching cycle. The red dot signifies the starting position. The molecular junction is then compressed (gray portion of curve) and stretched (black portion of curve). Once pulled beyond the starting position, the current drops, signifying the breaking of the dsDNA (red arrow). (b) Second cycle of compress/stretch experiment showing the compression (gray portion of curve) and stretching (black portion of curve) cycle. The drop in conductance for dsDNA molecular junctions is irreversible, supporting the force-induced melting model. (c) Two-dimensional logarithm of conductance *vs* tip displacement histogram showing three distinct regions of conductance behavior. The junction is either compressed (I), stretched (II), or broken (III).

CONCLUSION

In summary, we have investigated the effect of mechanical stretching on charge transport in dsDNA in an aqueous environment. The resistance of dsDNA is found to be linearly proportional to molecular length over a wide range, which supports the thermally activated hopping model, and the relatively small slope indicates long-range charge transport in DNA. The distance over which a dsDNA can be stretched before an abrupt decrease in the conductance is short and its

dependence on molecular length is weak. Furthermore, by repeatedly stretching and compressing the molecule, we have found that the abrupt decrease in conductance is an irreversible process. These observations indicate that mechanical stretching in dsDNA is localized near the ends of the molecule, and breaking of the hydrogen bonds in the end base pairs is responsible for the force-induced abrupt conductance decrease. Our results are in good agreement with experiments, theories, and simulations of mechanical properties of dsDNA. On the basis of this model, we found that the shear force to break the hydrogen bonds in the end base pairs is ~3 pN, and the spring constants of the end base pairs are ~70 times softer than the those in the middle of the dsDNA.

METHODS

DNA Sample Preparation. HPLC-purified oligonucleotide molecules used in this study were purchased from Integrated DNA Technologies. The oligonucleotide samples under investigation here ranged in length from 6 to 26 bases. The nucleic acid sequence for the molecules studied is 5′-A-$(CG)_N$-T-3′, where *N* ranged from 2 to 12, and was purchased with a thiol linker (3′-thiol modifier C3 S−S). This thiol linker was protected with a mercaptopropanol disulfide group during shipment and storage. Upon receipt of the samples, the oligonucleotides were suspended in 18 MΩ DI water for a concentration of 100 μM. This sample was then stored at −20 °C. Prior to conductance experiments, phosphate buffer solution (pH = 7.0) was prepared with 100 mM Na^+ and 10 mM tris(2-carboxyethyl)phosphine (TCEP) concentration. The target molecular sample was added to this solution to reach an oligo concentration of 20 μM and allowed to react for ~3 h at room temperature. The sample was then transferred to a spin column (Roche Applied Science quick spin column sephadex G-25) and centrifuged to remove the TCEP and mercaptopropanol. Phosphate buffer (pH = 7.0) containing 10 mM Mg^{2+} was then added to the deprotected sample to get a final oligo concentration of 10 μM. Mg^{2+} can help prevent the formation of hairpin structures for long DNA sequences, as was seen using 10% native polyacrylamide gel electrophoresis (see Supporting Information). As a result, it was not possible to measure conductance in samples longer than 14 bases without adding magnesium before annealing. The samples were then annealed in a thermal cycler by heating to 95 °C and cooling gradually to 4 °C over 4 h. The samples were kept at 4 °C until break junction measurements were performed. All break junction experiments were performed in phosphate buffer containing 10 mM Mg^{2+} and 10 μM dsDNA target molecule at room temperature.

STM Break Junction Sample Preparation and Measurement. The STM substrates used here were prepared in-house by thermally evaporating 1300 Å of gold (99.9999% purity, Alfa Aesar) onto freshly cleaved mica slides and annealed in vacuum to produce Au(111) surfaces. These substrates were transferred into individual vials and stored under vacuum until prior to measurement. Prior to adding the sample, the substrates were flame-annealed to clean and anneal the surface with a hydrogen flame. The STM tips used were produced by mechanically cutting gold wire and coating with Apiezon wax to reduce the leakage current during measurements in the aqueous environment.

The break junction experiments were performed using a Digital Instruments Nanoscope IIIA controller. A Molecular Imaging STM head and scanner were used to collect current and control tip motion. For all experiments described here, the current preamplifier used had a gain of 10 nA/V and the piezosensitivity in the *z*-axis was 3.9 nm/V. A custom-designed Labview (National Instruments) program, installed on an external computer, was used to perform the break junction experiments and collect the data discussed in this report. During all break junction and stretching−compression cycle experiments, the tip was moved at a ramp rate of 5 V/s, resulting in a stretching rate of ~20 nm/s. For break junction experiments, the STM tip was approached to the surface until the measured current reached the amplifier maximum (~100 nA). After reaching this current, the tip was further extended toward the surface for ~30 ms in order to make contact between the tip and surface. The tip was then retracted while measuring the tip−substrate current to produce conductance *versus* tip displacement curves. The stretching−compression cycle experiments were carried out using an algorithm to detect molecular junctions in real time, which is described elsewhere.[36] The stretching length is measured by processing the break junction data (conductance *vs* tip displacement decay curves) in a home-built Labview (National Instruments) program which measures the length of the molecular conductance plateau within a preset range. Molecular conductance histograms were constructed using all conductance *versus* tip displacement curves which showed a plateau; that is, the stretching length is not considered as a selection parameter for the conductance histogram. In constructing the stretching length histogram, the plateau lengths of molecular junctions which have conductance values within the full width at half-maximum of the conductance histogram are analyzed. The resulting stretching lengths for thousands of molecular junctions were then added into a histogram. Gaussian fittings for all histograms were performed in Origin 8.0 (OriginLab). Conductance and stretching length histograms were measured at least three times for each molecule studied, and the mean value among the different experiments was used for the molecule conductance (stretching length), with the standard deviation between different measurements used as the error in Figures 1d and 3b.

Conflict of Interest: The authors declare no competing financial interest.

Acknowledgment. The authors wish to thank Angela Edwards and Professor Hao Yan for help on the PAGE gel experiments, Professors Ratner and Mujica for support and discussions, and ONR (N00014-11-1-0729) for financial support.

Supporting Information Available: Additional stretching length data for alkanedithiol molecules and amine-terminated DNA molecules, more compression/stretching data, and sample preparation controls are provided online. This material is available free of charge *via* the Internet at http://pubs.acs.org.

REFERENCES AND NOTES

1. Kanvah, S.; Joseph, J.; Schuster, G. B.; Barnett, R. N.; Cleveland, C. L.; Landman, U. Oxidation of DNA: Damage to Nucleobases. *Acc. Chem. Res.* **2010**, *43*, 280–287.
2. Rajski, S. R.; Jackson, B. A.; Barton, J. K. DNA Repair: Models for Damage and Mismatch Recognition. *Mutat. Res.* **2000**, *447*, 49–72.
3. Garibotti, A. V.; Knudsen, S. M.; Ellington, A. D.; Seeman, N. C. Functional DNAzymes Organized into Two-Dimensional Arrays. *Nano Lett.* **2006**, *6*, 1505–1507.
4. Murphy, C. J.; Arkin, M. R.; Ghatlia, N. D.; Bossmann, S.; Turro, N. J.; Barton, J. K. Fast Photoinduced Electron Transfer through DNA Intercalation. *Proc. Natl. Acad. Sci. U.S.A.* **1994**, *91*, 5315–5319.
5. Lewis, F. D.; Liu, X.; Liu, J.; Miller, S. E.; Hayes, R. T.; Wasielewski, M. R. Direct Measurement of Hole Transport Dynamics in DNA. *Nature* **2000**, *406*, 51–53.
6. Giese, B.; Amaudrut, J.; Kohler, A.; Spormann, M.; Wessely, S. Direct Observation of Hole Transfer through DNA by Hopping between Adenine Bases and by Tunnelling. *Nature* **2001**, *412*, 318–320.

7. Xu, B.; Zhang, P.; Li, X.; Tao, N. Direct Conductance Measurement of Single DNA Molecules in Aqueous Solution. *Nano Lett.* **2004**, *4*, 1105–1108.
8. Van Zalinge, H.; Schiffrin, D. J.; Bates, A. D.; Starikov, E. B.; Wenzel, W.; Nichols, R. J. Variable-Temperature Measurements of the Single-Molecule Conductance of Double-Stranded DNA. *Angew. Chem., Int. Ed.* **2006**, *45*, 5499–5502.
9. Kang, N.; Erbe, A.; Scheer, E. Electrical Characterization of DNA in Mechanically Controlled Break-Junctions. *New J. Phys.* **2008**, *10*, 023030.
10. Song, B.; Elstner, M.; Cuniberti, G. Anomalous Conductance Response of DNA Wires under Stretching. *Nano Lett.* **2008**, *8*, 3217–3220.
11. Voityuk, A. A. Can Charge Transfer in DNA Significantly Be Modulated by Varying the π Stack Conformation? *J. Phys. Chem. B* **2009**, *113*, 14365–14368.
12. Wolter, M.; Woiczikowski, P. B.; Elstner, M.; Kubař, T. Response of the Electric Conductivity of Double-Stranded DNA on Moderate Mechanical Stretching Stresses. *Phys. Rev. B* **2012**, *85*, 075101.
13. Cluzel, P.; Lebrun, A.; Heller, C. DNA: An Extensible Molecule. *Science* **1996**, *271*, 792–794.
14. Smith, S. B. S.; Cui, Y.; Bustamante, C. Overstretching B-DNA: The Elastic Response of Individual Double-Stranded and Single-Stranded DNA Molecules. *Science* **1996**, *271*, 795–799.
15. Baumann, C. G.; Smith, S. B.; Bloomfield, V. A.; Bustamante, C. Ionic Effects on the Elasticity of Single DNA Molecules. *Proc. Natl. Acad. Sci. U.S.A.* **1997**, *94*, 6185–6190.
16. Lebrun, A.; Lavery, R. Modelling Extreme Stretching of DNA. *Nucleic Acids Res.* **1996**, *24*, 2260–2267.
17. Rouzina, I.; Bloomfield, V. A. Force-Induced Melting of the DNA Double Helix 1. Thermodynamic Analysis. *Biophys. J.* **2001**, *80*, 882–893.
18. King, G. A.; Gross, P.; Bockelmann, U.; Modesti, M.; Wuite, G. J. L.; Peterman, E. J. G. Revealing the Competition between Peeled ssDNA, Melting Bubbles, and S-DNA during DNA Overstretching Using Fluorescence Microscopy. *Proc. Natl. Acad. Sci. U.S.A.* **2013**, *110*, 3859–3864.
19. Zhang, X.; Chen, H.; Le, S.; Rouzina, I.; Doyle, P. S.; Yan, J. Revealing the Competition between Peeled ssDNA, Melting Bubbles, and S-DNA during DNA Overstretching by Single-Molecule Calorimetry. *Proc. Natl. Acad. Sci. U.S.A.* **2013**, *110*, 3865–3870.
20. Hatch, K.; Danilowicz, C.; Coljee, V.; Prentiss, M. Demonstration That the Shear Force Required To Separate Short Double-Stranded DNA Does Not Increase Significantly with Sequence Length for Sequences Longer than 25 Base Pairs. *Phys. Rev. E* **2008**, *78*, 011920.
21. Roe, D. R.; Chaka, A. M. Structural Basis of Pathway-Dependent Force Profiles in Stretched DNA. *J. Phys. Chem. B* **2009**, *113*, 15364–15371.
22. Wolter, M.; Elstner, M.; Kubař, T. On the Structure and Stretching of Microhydrated DNA. *J. Phys. Chem. A* **2011**, *115*, 11238–11247.
23. de Gennes, P.-G. Maximum Pull out Force on DNA Hybrids. *C. R. Acad. Sci., Ser. IV: Phys., Astrophys.* **2001**, *2*, 1505–1508.
24. Nath, S.; Modi, T.; Mishra, R. K.; Giri, D.; Mandal, B. P.; Kumar, S. Statistical Mechanics of DNA Rupture: Theory and Simulations. *J. Chem. Phys.* **2013**, *139*, 165101.
25. Xu, B.; Tao, N. J. Measurement of Single-Molecule Resistance by Repeated Formation of Molecular Junctions. *Science* **2003**, *301*, 1221–1223.
26. Luo, L.; Choi, S. H.; Frisbie, C. D. Probing Hopping Conduction in Conjugated Molecular Wires Connected to Metal Electrodes. *Chem. Mater.* **2011**, *23*, 631–645.
27. Chaurasiya, K. R.; Paramanathan, T.; McCauley, M. J.; Williams, M. C. Biophysical Characterization of DNA Binding from Single Molecule Force Measurements. *Phys. Life Rev.* **2010**, *7*, 299–341.
28. Saito, I.; Takayama, M.; Sugiyama, H.; Nakatani, K.; Tsuchida, A.; Yamamoto, M. Photoinduced DNA Cleavage via Electron Transfer: Demonstration That Guanine Residues Located 5′ to Guanine Are the Most Electron-Donating Sites. *J. Am. Chem. Soc.* **1995**, *117*, 6406–6407.
29. Nitzan, A. The Relationship between Electron Transfer Rate and Molecular Conduction. 2. The Sequential Hopping Case. *Isr. J. Chem.* **2002**, *42*, 163–166.
30. Conron, S. M. M.; Thazhathveetil, A. K.; Wasielewski, M. R.; Burin, A. L.; Lewis, F. D. Direct Measurement of the Dynamics of Hole Hopping in Extended DNA G-Tracts. An Unbiased Random Walk. *J. Am. Chem. Soc.* **2010**, *132*, 14388–14390.
31. Genereux, J. C.; Barton, J. K. Mechanisms for DNA Charge Transport. *Chem. Rev.* **2010**, *110*, 1642–1662.
32. Noy, A.; Vezenov, D. V.; Kayyem, J. F.; Meade, T. J.; Lieber, C. M. Stretching and Breaking Duplex DNA by Chemical Force Microscopy. *Chem. Biol.* **1997**, *4*, 519–527.
33. Rubio, G.; Agraït, N.; Vieira, S. Atomic-Sized Metallic Contacts: Mechanical Properties and Electronic Transport. *Phys. Rev. Lett.* **1996**, *76*, 2302–2305.
34. Huang, Z.; Chen, F.; Bennett, P. A.; Tao, N. Single Molecule Junctions Formed via Au–Thiol Contact: Stability and Breakdown Mechanism. *J. Am. Chem. Soc.* **2007**, *129*, 13225–13231.
35. Arroyo, C. R.; Leary, E.; Castellanos-Gómez, A.; Rubio-Bollinger, G.; González, M. T.; Agraït, N. Influence of Binding Groups on Molecular Junction Formation. *J. Am. Chem. Soc.* **2011**, *133*, 14313–14319.
36. Guo, S.; Hihath, J.; Díez-Pérez, I.; Tao, N. Measurement and Statistical Analysis of Single-Molecule Current–Voltage Characteristics, Transition Voltage Spectroscopy, and Tunneling Barrier Height. *J. Am. Chem. Soc.* **2011**, *133*, 19189–19197.
37. Fu, H.; Chen, H.; Marko, J. F.; Yan, J. Two Distinct Overstretched DNA States. *Nucleic Acids Res.* **2010**, *38*, 5594–5600.
38. Bosaeus, N.; El-Sagheer, A. H.; Brown, T.; Smith, S. B.; Akerman, B.; Bustamante, C.; Nordén, B. Tension Induces a Base-Paired Overstretched DNA Conformation. *Proc. Natl. Acad. Sci. U.S.A.* **2012**, *109*, 15179–15184.